Quaternary Science Reviews 280 (2022) 107413

Contents lists available at ScienceDirect

Quaternary Science Reviews

journal homepage: www.elsevier.com/locate/quascirev

Half-precession signals in Lake Ohrid (Balkan) and their spatio-temporal relations to climate records from the European realm

Arne Ulfers [a, *], Christian Zeeden [a], Silke Voigt [b], Mehrdad Sardar Abadi [a], Thomas Wonik [a]

[a] Leibniz Institute for Applied Geophysics, Stilleweg 2, 30655, Hannover, Germany
[b] Institute of Geosciences, Goethe University Frankfurt, Altenhöferallee 1, 60438, Frankfurt, Germany

ARTICLE INFO

Article history:
Received 30 June 2021
Received in revised form
14 December 2021
Accepted 31 January 2022
Available online 17 February 2022

Handling Editor: A. Voelker

ABSTRACT

The nature of half-precession (HP) cycles (~9000–12,000 years), although identified in numerous records, is still poorly understood. Here we focus on HP signals in Lake Ohrid and in a variety of different marine and terrestrial proxy records from Europe and the Northern Atlantic region. Our study examines the temporal evolution of the HP signal from the early/middle Pleistocene to the present, discusses the results across the latitudes of the Mediterranean and Europe, and assesses the potential of the HP to reflect the connectivity of climate systems over time.

We apply filters on the datasets that remove the classical orbital cycles (eccentricity, obliquity, precession) and high frequency signals to focus exclusively on the bandwidth of the HP signal. Evolutionary wavelet spectra and correlation techniques are used to study the evolution of frequencies through the different records.

Next to a connection of HP cycles to interglacials, we see a more pronounced HP signal in the younger part of several proxy records. Although the HP signal is present in all of the investigated sites, we observe a more pronounced HP signal in the southeast compared to records from the north. The latter is consistent with the assumption that HP is an equatorial signal and can be transmitted northward via various pathways. The appearance of HP signals in mid- and high-latitude records can thus be an indicator for the intensity of the mechanisms driving these pathways. The African Monsoon probably plays a major role in this context, as its magnitude directly influences the climate systems of the Mediterranean and Southern Europe.

1. Introduction

1.1. Characteristics of half-precession cycles and state of the art

After Milutin Milanković published his theories on orbital cycles in the first half of the 20th century, it took decades until these were accepted as catalysts for warm/cold periods (Milanković, 1920, 1941; Hays et al., 1976). Since then, major progress was made in cyclostratigraphy and the impact of orbital forcing on the climate system (e.g. Weedon, 2003; Hinnov, 2000 and references therein). Most studies focused on the role of the three major cycles (eccentricity, obliquity, precession), while sub-Milanković frequencies (less than 15 ka) usually received only secondary attention. In this study, we specifically address cycles between 12 and 9 ka. This frequency band, referred to as half-precession (HP), is a harmonic of the 23–19 ka precession cycles (Berger et al., 1997). The HP signal is considered to be most intense in the intertropical zone, as it results from the twice-yearly passage of the sun across the equator (Short et al., 1991; Berger et al., 2006). Studies on marine records first proved the occurrence of HP (e.g. Hagelberg et al., 1994; Hinnov et al., 2002). HP cycles were also described as a response to monsoon rainfall in lacustrine records from Africa (Trauth et al., 2003; Verschuren et al., 2009; Scholz et al., 2007). Deposits from the Chinese Loess Plateau suggest that mid-latitude terrestrial records are able to reflect HP signals which originate from the East Asian summer monsoon in the tropical Pacific Ocean (Sun and Huang, 2006). Similar observations about the HP signal were made by Turney et al. (2004) who suggest that climate variations in the tropical Pacific Ocean exert an influence on North Atlantic climate through atmospheric and oceanic teleconnections on

* Corresponding author.
E-mail addresses: Arne.Ulfers@leibniz-liag.de (A. Ulfers), Christian.Zeeden@leibniz-liag.de (C. Zeeden), s.voigt@em.uni-frankfurt.de (S. Voigt), Mehrdad.SardarAbadi@leibniz-liag.de (M. Sardar Abadi), Thomas.Wonik@leibniz-liag.de (T. Wonik).

https://doi.org/10.1016/j.quascirev.2022.107413

orbital timescales. In comparison to marine records, terrestrial records (lacustrine and loess) are usually relatively short. The longest terrestrial record mentioned in the references above has an age of 175 ka (Trauth et al., 2003), while marine records often span longer periods with millions of years (e.g. Hagelberg et al., 1994; Grant et al., 2017). Controversy is still ongoing about how HP affects climate and is transferred into geological records (Hinnov et al., 2002; De Vleeschouwer et al., 2012, and references therein). In this context, it is important to recognize that insolation forcing is only one step in an astronomical theory of paleoclimate (Berger et al., 2006), and that astronomical climate forcing can act nonlinear and complex (e.g. Meyers, 2019; Liebrand and de Bakker, 2019).

1.2. Aim of the study

HP is observable in various marine (e.g. Hagelberg et al., 1994; Grant et al., 2017) as well as terrestrial records (e.g. Antoine et al., 2013; Colcord et al., 2018) but is often not described in detail or further investigated (e.g. Hodell et al., 2013). In some of the just referenced records and Lake Ohrid data (see chapter 1.3 'Setting of Lake Ohrid'), HP cycles are very distinctly developed.

In our study, we use various proxy records in and around Europe to characterize and quantify the HP signal. We (1) investigate HP cycles in Lake Ohrid and (2) set the results in temporal and spatial connection to other records containing clear HP cyclicity. We observe HP over a period of more than 1 Ma in Lake Ohrid and in other long-term records with (in)direct impact of climate systems influencing Europe. Further, we show that HP is also present in high-latitude records, even if not very pronounced and/or superimposed by the main orbital cycles (eccentricity, obliquity, precession). We assess the influence of HP on records from Europe and surrounding regions with the aim to better understand its spatial and temporal occurrence. Assuming that the HP signal originates in tropical regions (Hagelberg et al., 1994; Short et al., 1991), its influence on Europe is largely determined by how the signal is carried northward. As an example, the Nile River transmits information from tropical Africa to the Mediterranean Sea (e.g. Rohling et al., 2015; Rossignol-Strick, 1985). The occurrence of HP in mid-to high-latitudes can thus be used as a measure of connectivity between tropical and subtropical/temperate/subpolar climate zones in the past.

1.3. Setting of Lake Ohrid

Lake Ohrid is located on the Balkan Peninsula between Albania and North Macedonia. It is considered Europe's oldest lake, and therefore it is a valuable archive for studies that focus on changes in local (hydro)climate during the last ~1.36 Ma (e.g. Wagner et al., 2014, 2019). Simplified, the succession consists of two types of hemipelagic sediments: calcareous silty clay deposited during interglacials and clastic, silty clay deposited during glacials (Francke et al., 2016). Several layers of volcanic ash allow tephrostratigraphic analyses, which are the basis for the development of a robust age-depth model besides the borehole logging data (Leicher et al., 2016; Wagner et al., 2019; Ulfers et al., 2022).

The present day climate around Lake Ohrid is mostly a Mediterranean type climate with hot/arid summers and typically rainfall maxima during mild winters (Schemmel et al., 2016). The principal climate systems of the region are highlighted in Fig. 1. There is a pronounced sensitivity to the variability of atmospheric circulation patterns, such as the Siberian High intensity, the North Atlantic Oscillation modes (NAO^+/NAO^-), and the monsoon systems (e.g. Schemmel et al., 2016; Lionello et al., 2012; Wanner et al., 2001). Southward displacement of the westerly track reflects growth of the Fennoscandian ice sheet (Ünal-İmer et al., 2015). Proxy records from Lake Ohrid and climate models suggest that North Atlantic low-pressure systems entering the Mediterranean Sea are strengthened during periods of low continental ice volume. This increases the winter rainfall in the Mediterranean Sea (Wagner et al., 2019; Kutzbach et al., 2014). Wagner et al. (2019) also demonstrate a connection of Lake Ohrid's precipitation proxies with Mediterranean sapropels. The latter are organic rich layers in marine sediments which indicate enhanced African monsoons activity (e.g. Rohling et al., 2015; Rossignol-Strick, 1985).

2. Material and Methods

2.1. Data description and pre-processing

Multi-proxy studies as from Li et al. (2019) are of significant value as they allow to assess the individual suitability of a proxy to reflect astronomical forcing. The records used in this study include a variety of proxies, time intervals, and locations around Europe and the North Atlantic.

The datasets from Lake Ohrid are from an ICDP drilling campaign in 2013. Geophysical downhole logging was conducted by the Leibniz Institute for Applied Geophysics and several continuous data sets of physical properties were obtained. The parameters used in this study are gamma radiation (GR, including concentrations of U, K, Th) and magnetic susceptibility (MS), each with a vertical resolution of 10–20 cm. Principals of logging techniques are described in Rider and Kennedy (2011), details about the logging procedure in Lake Ohrid are given by Baumgarten et al. (2015). Pre-processing of data was performed with the GeoBase® (Antares, Germany) and WellCAD® software (Advanced Logic Technology, Luxembourg). The GR in Lake Ohrid is connected to detrital input of clay minerals, which contain radioactive elements like U, K and Th. The detrital input is higher in glacials due to increased erosion in the hinterland caused by reduced vegetation (Vogel et al., 2010).

Core based analyses of sediments from Lake Ohrid are obtained after the creation of a composite record. The proxies used in this study are listed in Table 1. Total inorganic carbon (TIC) and total organic carbon (TOC) contents were determined at the University of Cologne and relative quartz concentrations (Qz) at the University of Bern using Fourier transform infrared spectroscopy.

The majority of carbonates in the sediments of Lake Ohrid is endogenous calcite, which is formed predominantly by the photosynthetically induced formation of calcite crystals in the epilimnion. The precipitation occurs at warm temperatures, as long as Ca^{2+} and HCO_3^- ions are available (Francke et al., 2016; Vogel et al., 2010). This supply is provided during interglacials by increased karst flow through the mountains consisting of limestone east of Lake Ohrid. The source of the increased hydrological pressure is the elevated Lake Prespa on the eastern side of the mountain range (Wagner et al., 2010).

Palynological investigations were conducted by several investigators across European laboratories. Deciduous oak pollen represent the combined percentages of *Quercus robur* and *Quercus cerris* types (Q.dec), which are commonly used as an indicator for mid-elevation, relatively humid forest across the Mediterranean. Relative abundances of arboreal pollen excluding *Pinus* pollen (AP.Pin) are based on the sum of the total terrestrial pollen excluding *Pinus* owing to overrepresentation and potential long-distance transport of this taxon. In general, pollen abundance decreases in glacials (Sadori et al., 2016; Wagner et al., 2019; Hooghiemstra, 2006).

Additionally, we use datasets with various climate-sensitive proxies in the European and North Atlantic regions for

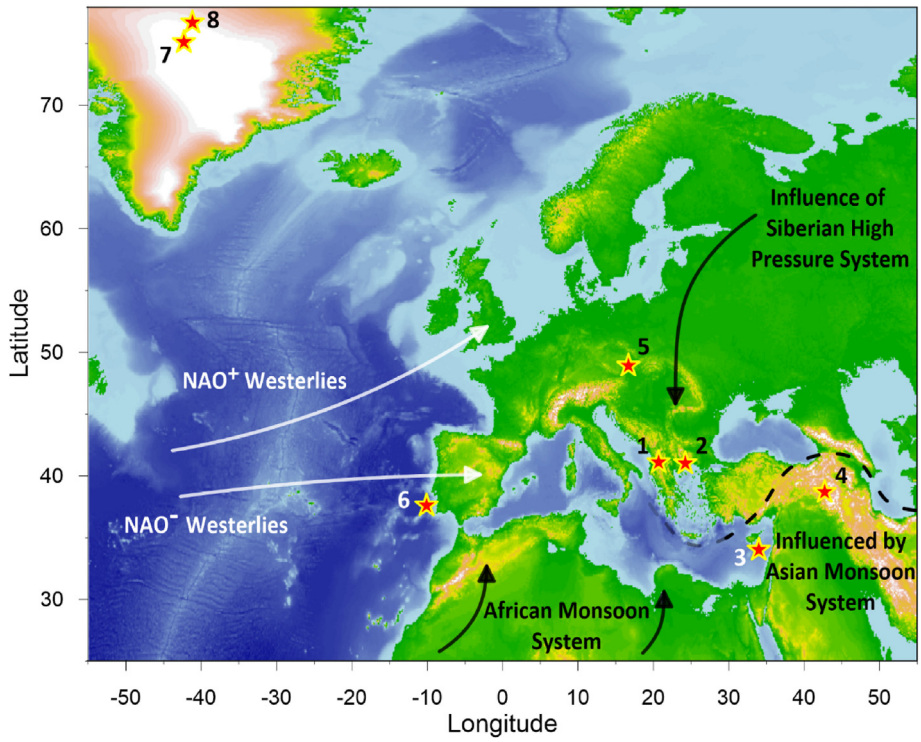

Fig. 1. Overview of data locations used in this study. Schematic atmospheric circulation patterns affecting the Mediterranean are indicated by arrows (after Schemmel et al., 2016). Dashed line represents influence of Asian Monsoon Systems. North Atlantic Oscillation (NAO) in positive and negative mode influencing the Westerlies and thus heat and moisture transport towards the Mediterranean (for details see Wanner et al., 2001). Selected sites have met at least one of the following criteria: Possibly covering long time intervals, sufficient resolution to record half-precession cycles, obvious presence of half-precession cycles and data availability. 1. Lake Ohrid, Albania/North Macedonia; 2. Tenaghi Philippon, Greece; 3. ODP Site 967, Eastern Mediterranean; 4. Lake Van, Turkey; 5. Dolní Věstonice, Czech Republic; 6. IODP Site U1385 "Shackleton site", Iberian Margin; 7. NGRIP, Greenland; 8. Synthetic record, Greenland; there is no position given in the synthetic record, we therefore use the center of Greenland for latitude dependent analysis with this record (see Table 1 for details). Map data are from the US National Oceanic and Atmospheric Administration (NOAA; Amante and Eakins, 2009).

comparison with the Lake Ohrid records (Table 1; Fig. 1). The wet-dry index from ODP expedition 967 in the Eastern Mediterranean is a combination of a sapropel/monsoon run-off proxy yielded by XRF data and a dust record from the same site. This results in a new index for changes in relative humidity and aridity in Northwest Africa (Grant et al., 2017; Larrasoaña et al., 2003). The Ca/Ti ratio measured in cores from the Iberian Margin is a proxy that reflects relative changes of biogenic carbonate and detrital sediment, whereas biogenic carbonate is increased during interglacials (Hodell et al., 2015; Thomson et al., 1999). The Greenland synthetic temperature record (GL_T_syn) is based on the thermal bipolar seesaw model, which proposes opposite temperature responses in the two hemispheres (Broecker, 1998; Stocker and Johnsen, 2003). Temperature changes are estimated using methane-tuned temperature records from Greenland and Antarctica to reconstruct the Greenland records beyond the present limit (Barker et al., 2011). The total organic carbon content in Lake Van (L.Van.TOC) is connected to productivity and lake level fluctuations. Both are associated with glacial-interglacial variability, with increased TOC during warmer/wetter periods as a result of higher lake levels and increased productivity (Stockhecke et al., 2014b). For more details about paleoenvironmental characteristics of the proxies from Table 1, please see references therein.

Most of the analyzed records spans over more than the last 1 Ma (Tab. 1). Each dataset has its own time resolution spanning from 0.05 ka in the synthetic temperature record from Greenland (GL_T_syn) to ~2 ka in the pollen records from Lake Ohrid (Q.dec and AP.Pin). Several utilized methods require equally spaced sampling in time. This is why we interpolate each dataset to its individual mean resolution for further analysis. We utilize the age-models created in the original studies listed in Table 1 (see references therein for details about methods of age-model construction).

2.2. Time series analysis

For data analyses we use the 'astrochron' package for the open-source software 'R' (Meyers et al., 2021; R Core Team, 2021). The R code is provided as Supplement Material 02.

We perform wavelet analyses according to the method of Torrence and Compo (1998) and Liu et al. (2007) using a Morlet mother wavelet. As described above, the datasets are evenly spaced, each at its individual mean resolution. To emphasize the focus on the HP signal, our plots cover only the periodicities between 25 ka to 4 ka.

We apply a Taner bandpass filter (Taner, 1992) to all datasets in the time domain. Taner filters are well established in the field of cyclostratigraphy as they are convenient to apply and filter properties can be adjusted precisely (Zeeden et al., 2018). The roll-off rate of Taner filters can be set steeply (in our case almost vertical at the cutoff frequency, Fig. 2), while the shape of e.g. Gaussian filters allows areas outside the edges of the cutoff frequencies to pass (Kodama and Hinnov, 2014). Given that the HP signal has a narrow bandwidth (12–9 ka), it is important for our study that this is sharply cut from other frequencies. The cutoff frequency of the used filters is set between 1/13 and 1/8.5. Fig. 2 illustrates the filter settings using the amplitude spectrum of GR in Lake Ohrid as an example. This proxy has already proven suitable in previous studies to characterize orbital cycles (Baumgarten et al., 2015; Ulfers et al., 2022). Spectra of Lake Ohrid: GR, K, TIC, Q.dec; Eastern Mediterranean, ODP wet-dry index; Lake Van, TOC; Iberian Margin, Ca/Ti

Table 1
Proxy datasets used in this study. The eight proxies highlighted in bold are discussed and displayed in more detail (e.g. Figs. 3 and 4). All other records are shown in the Supplement Material 01. *This is not a generalization, but valid for the listed site (i.e. in Lake Ohrid GR is a proxy for detrital input). The proxy descriptions are simplified. For details see the corresponding references.

Site	Parameter	Abbreviation	Proxy for*	Age [ka]	Reference
Lake Ohrid	**Gamma radiation**	**GR**	**Detrital input (high GR = high input)**	**0 −1081**	Baumgarten et al. (2015) Ulfers et al. (2022)
Lake Ohrid	Uranium concentration	U	Detrital input (high U = high input. May be biased by organic matter (TOC)	0 −1081	Ulfers et al. (2022)
Lake Ohrid	**Potassium concentration**	**K**	**Detrital input (high K = high input)**	**0 −1081**	Baumgarten et al. (2015) Ulfers et al. (2022)
Lake Ohrid	Thorium concentration	Th	Detrital input (high Th = high input)	0 −1081	Ulfers et al. (2022)
Lake Ohrid	Magnetic susceptibility	MS	Magnetic minerals (may be biased by diagenetic processes	61 −1081	Ulfers et al. (2022)
Lake Ohrid	**Total inorganic carbon**	**TIC**	**Hydrology (high TIC = high temperature and/or karst runoff)**	**1 −1364**	Wagner et al. (2019)
Lake Ohrid	Total organic carbon	TOC	Biologic productivity and organic matter delivery and burial	1 −1364	Wagner et al. (2019)
Lake Ohrid	Relative sedimentary quartz	Qz	Detrital input (high Qz = high detrital input).	2 −1363	Wagner et al. (2019)
Lake Ohrid	**Deciduous oak pollen (Q.dec)**	**Q.dec**	**Vegetation catchment (indicator for mid-elevation, relatively humid forest)**	**0 −1362**	Wagner et al. (2019)
Lake Ohrid	Arboreal pollen without Pinus	AP.Pin	Vegetation catchment	0 −1362	Wagner et al. (2019)
Greece - Tenaghi Philippon	Arboreal pollen	TPhi.AP	Vegetation catchment	0 −1101	Tzedakis et al. (2006)
East. Mediterranean - ODP 967	**ODP wet-dry index**	**wet-dry index**	**Relative humidity and aridity**	**4 −3000**	Grant et al. (2017)
Turkey - Lake Van	**Total organic carbon**	**L.Van.TOC**	Biologic productivity and organic matter delivery and burial	**1–264**	Stockhecke et al. (2014a)
Czech Republic - Dolní Věstonice	Magnetic susceptibility	DolVes.MS	Aeolian sedimentation and loess deposits	22 −126	Antoine et al. (2013)
Atlantic - Iberian Margin	Sea surface temperature	IbM.SST	Temperature	0 −1017	Rodrigues et al. (2017)
Atlantic - Iberian Margin	**Ca/Ti**	**IbM.Ca/Ti**	**Detrital input and bioproductivity**	**0 −1429**	Hodell et al. (2015)
Greenland	$\delta^{18}O$	NGRIP.$\delta^{18}O$	Temperature	0–120	NGRIP members, 2004
Greenland	**Synthetic temperature variability**	**GL_T_syn**	**Temperature**	**5–798**	Barker et al. (2011)

and Greenland, synthetic temperature, are included in Supplementary Material 03. Even if the HP signal in Fig. 2 does not appear obvious at first view, there are several peaks above the AR(1) 99% confidence level in Fig. 2b. Additional information on the detection of the HP signal and its significance is provided in Supplementary Material 04, again using the example of GR in Lake Ohrid.

Subsequently we create an envelope for the filtered signal using the Hilbert transform function. The envelope is then smoothed using a Taner low-pass filter with a cutoff frequency of 0.0125 (≙ 80 ka). This filter will omit high-frequency amplitude components not related to eccentricity, but capture all eccentricity components (here the ~100 ka and ~405 ka) to allow a reasonable comparison with eccentricity as from the calculations of Laskar et al. (2004).

We determine the Pearson correlation coefficients between the original data and the Taner-filtered signal to provide a quantitative evaluation of the HP signal in the stratigraphic series. This is conducted using the 'surrogateCor' function, which is included in the 'R' package 'astrochron' (Meyers, 2014; R Core Team, 2021). The statistical significance of the obtained coefficients is assessed using 1000 Monte Carlo simulations. We use this method for entire records as well as for intervals of special interest (e.g. the time after the Mid-Pleistocene Transition). We employ the same approach to determine the correlation between eccentricity and the filtered signal from the Hilbert envelope.

To illustrate how the correlation between the original data and the Taner-filtered signal (and thus the clarity of the HP cycle) evolve with time, we use the moving window cross-correlation after Sageman and Hollander (1999). In this method, two stratigraphic series are compared using a certain window size. In our study we select a 100-ka-window to display the long-term evolution of the HP signal.

3. Results

3.1. Wavelet analysis

The results of the wavelet analyses of the eight highlighted records in Table 1 are given in Fig. 3. A compilation of all examined records is available in Supplement Material 05. In many records, clear precession signals (period between 19 and 23 ka; e.g., in Fig. 3e and g) or high-frequency signals (period <8 ka; e.g., Fig. 3g and h) are evident. The focus in this study is on the frequency range of HP (9–12 ka), indicated by the white dashed lines in Fig. 3.

Within the last 1 Ma, the HP signal in the different proxy records reveals quite different characteristics. In the borehole data (Fig. 3a and b), we observe that a distinct HP signal is visible more common in interglacials (e.g. MIS 15, 13, 11, 7). This pattern is even more evident in the core data from Lake Ohrid (Fig. 3c and d). In particular in the TIC record, one can observe a direct link of the HP signal to interglacials and its disappearance in glacials.

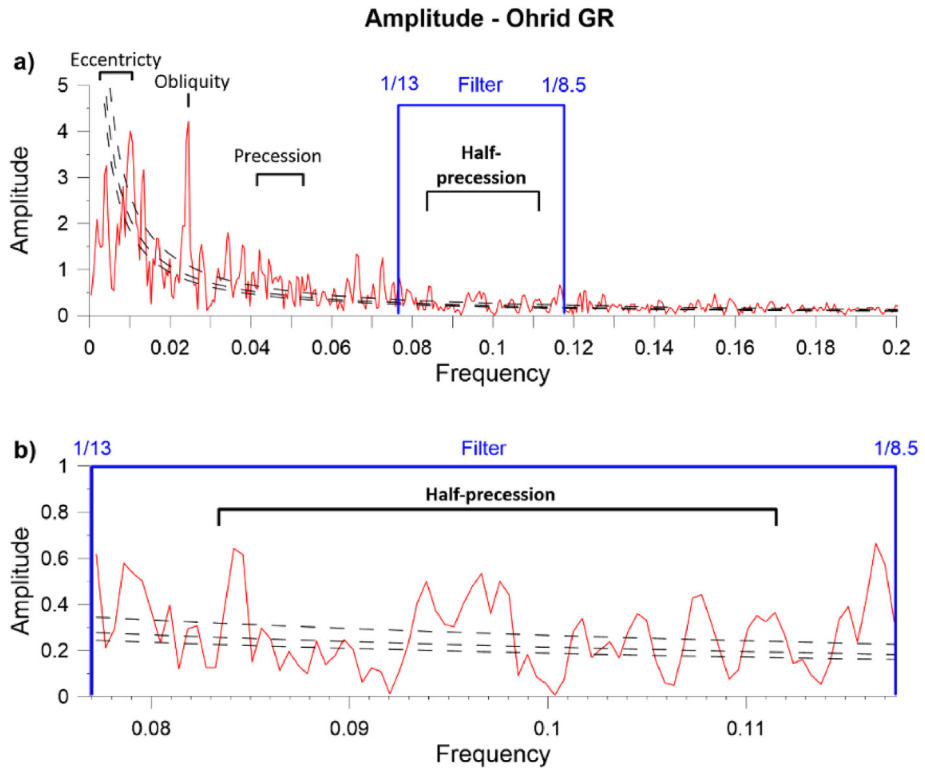

Fig. 2. Amplitude spectrum of gamma radiation record from Lake Ohrid. Filter settings in blue (13–8.5 ka) focusing on half-precession (12–9 ka). The filter is selected wider than HP's actual bandwidth to account for uncertainties. In a) with complete frequency range up to 0.2 (= 5 ka) including Milanković cycles. In b) focusing on the spectra within the filter settings. In both figures dashed lines from top to bottom represent AR(1), 99%, 95% and 90% confidence levels, respectively. The original data and the resulting filtered signal are displayed in Fig. 4a. All datasets examined in this study are filtered in this way, GR only serves as an example here. (For interpretation of the references to color in this figure legend, the reader is referred to the Web version of this article.)

The HP signal is also subject to (quasi-periodic) variations in the ODP wet-dry index (Fig. 3e). Even though the tendency is still towards a connection of HP and interglacials, there are glacials with clear HP signal as well (e.g. MIS 16 and 12). The TOC data from Lake Van is the shortest record presented here (Fig. 3f). The HP signal is most evident in MIS 11, in the transition from MIS 7/6, and MIS 5, i.e. mostly in interglacials. In the Ca/Ti record from the Iberian Margin (Fig. 3g) the HP signal is well recognizable, but a clear assignment to interglacials or glacials is not possible. For example, the two most prominent maxima are at the transition between MIS 13/12 and MIS 9/8. Pronounced minima are located in glacials (e.g., MIS 22, 18, 6), but there are also glacials with a strong HP signal (e.g., 20, 14, 12). In the record from Greenland, a clear connection of HP to glacial/interglacial variability is not visible. It looks as if the HP signal is permanently present in the record. However, this also applies to other periods (outside the range of HP). In particular, the low-frequency signals (<8 ka) are pronounced. The only slightly recognizable pattern is a tendency for the HP signal to be stronger in the interval younger than ~340 ka.

3.2. Correlative estimates

Fig. 4 shows a selection of investigated records from this study. Examining the original data (black lines), it is apparent that the amplitude variation of most proxies is increased in interglacials. For example, Lake Ohrid TIC hardly exhibits any variations during glacials. Although TIC is showing the common feature of "low-variability in glacials" particularly prominent, a similar pattern is present for most parameters, whether downhole-, geochemical-, pollen- or synthetic data.

Comparing the original data (black lines in Fig. 3) with the filtered signal (thin red lines), we can observe a similarity of strong peaks in some time intervals of all proxies. This is especially prominent during interglacials and in transitions from interglacials to glacials. A good example is MIS 13 and its transition into MIS 12, where several cycles with a period of 13–8.5 ka are visible in the GR, the K, the Q.dec and the Ibm.Ca/Ti (Fig. 4a, b and 4d; Supplement Material 01). Similar observations are made for MIS 7. Even though individual cycles in the original record are absent (e.g. in TIC at ~228 ka) or weak (in GR and IbM.Ca/Ti at ~228 ka), this is a good illustration of sub-Milanković cycles in interglacials. In some records, these cyclic patterns proceed into the next glacial as seen for example in MIS 6 (Q.dec, L.Van.TOC, and IbM.Ca/Ti; Fig. 4d, f and 4g).

The relation of eccentricity (Fig. 4i) to the signal of the filtered HP envelopes (Fig. 4, purple) is more complex and the respective proxy records have to be examined individually. In some parts, the amplitudes are in phase or just slightly offset. To give two examples of such a case, we point out to the Lake Ohrid GR between MIS 15–11, or to the younger section (<530 ka) of the IbM.Ca/Ti (Fig. 4a and g). Cases with no apparent correlation between eccentricity and filtered signal can be observed e.g. for Lake Ohrid K between MIS 11–5 or in wet-dry index between MIS 16–8 (Fig. 4b and e).

In Fig. 4, we qualitatively display some relationships between HP and orbital cycles. To quantify these relations, we determine the Pearson correlation coefficients for complete records or for intervals of particular interest (see chapter 2. 'Material and Methods'). The Pearson correlation coefficients between the original data (black lines in Fig. 4) and the Taner filtered signal (thin red lines in Fig. 4) for each entire record are listed in Fig. 5. When

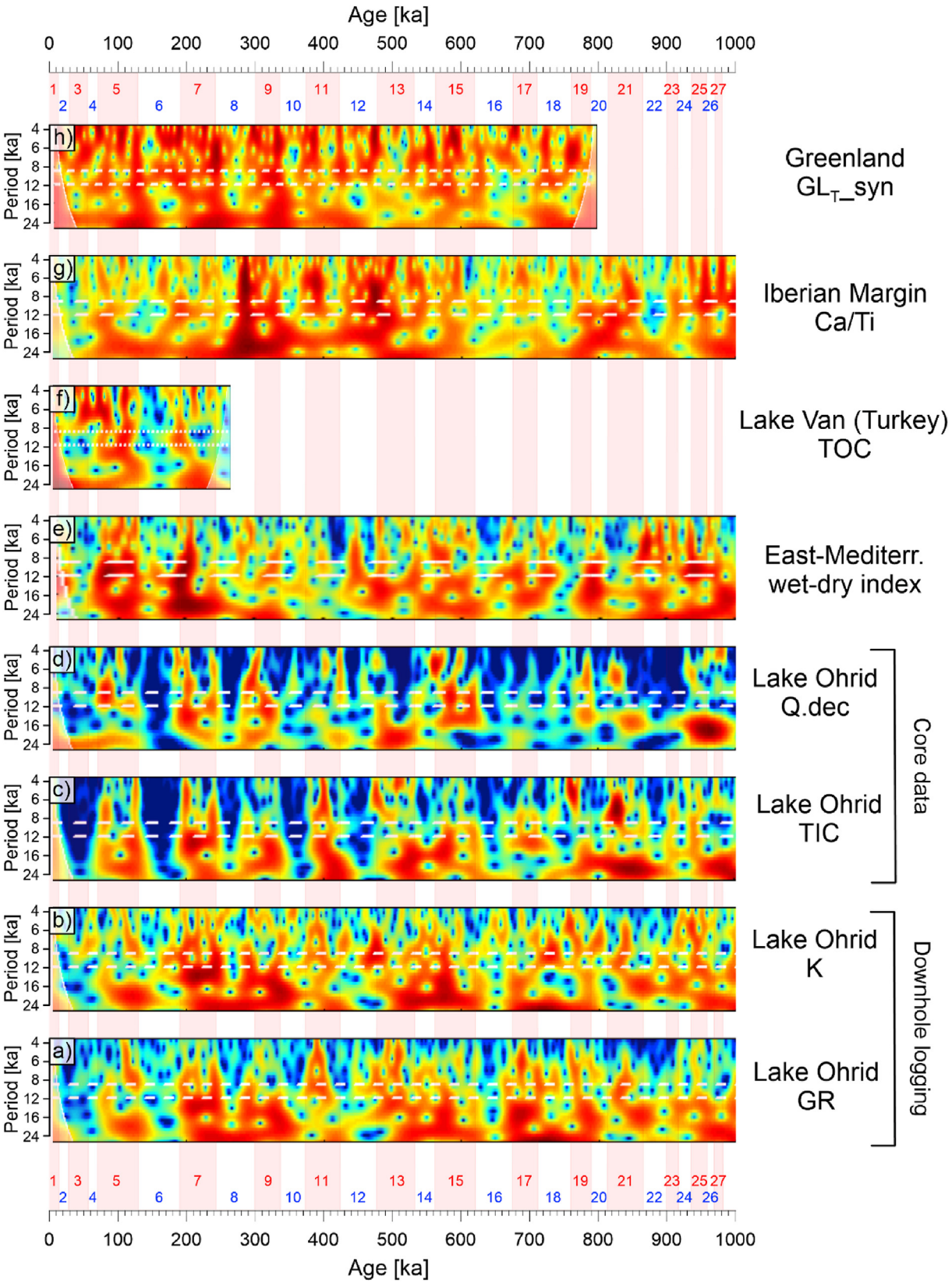

Fig. 3. Wavelet analyses for different proxy signals over the last 1 Ma. Marine isotope stages are indicated in red (interglacials) and blue (glacials) numbered above/below age axes. Reddish background color highlights interglacials. In all spectra high power is indicated by red color, while low power is blue. The period ranges from ~4 to 24 ka, thus even contains the precession signals. The interval of HP (9–12 ka) is located between the dashed white lines. Especially in core data from Lake Ohrid (c and d), the HP signal is stronger in interglacials compared to glacials. In the record from Greenland (h) no connectivity of the HP signal at a certain age is recognizable. All other records exhibit, at least partially, a relationship between HP and interglacials. (For interpretation of the references to color in this figure legend, the reader is referred to the Web version of this article.)

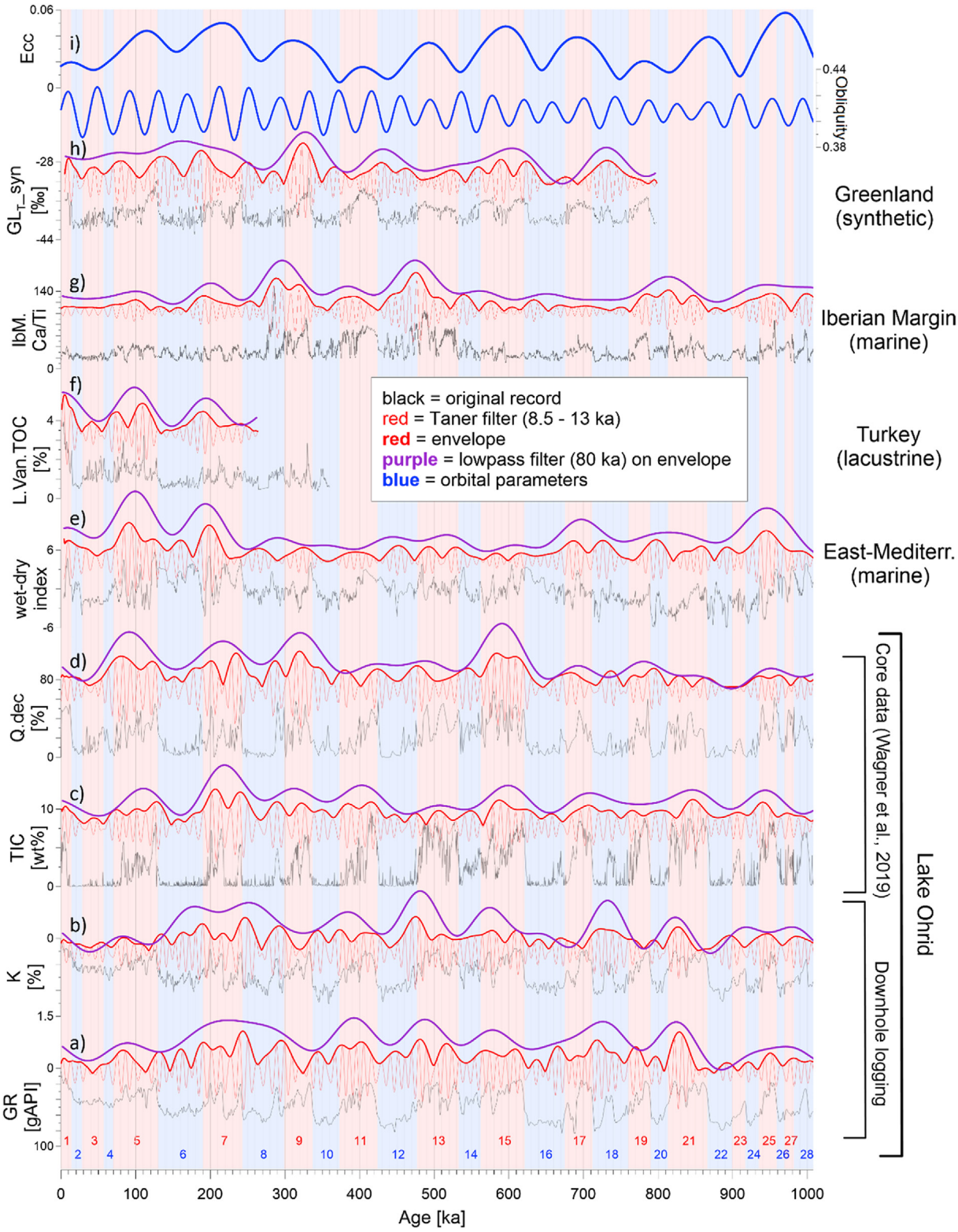

Fig. 4. Eight of the investigated records (GR, K, TIC, Q.dec, wet-dry index, L.Van.TOC, Ibm.Ca/Ti, GL_T_syn and obliquity, eccentricity) with original data (black), the signal after applying the bandpass filter (thin red line) and its envelope (thick red line). The purple line represents the lowpass-filtered envelope which omits high-frequency amplitude components not related to eccentricity (detailed information on filter settings in chapter 2. 'Material and Methods'). At the top are obliquity and eccentricity from Laskar et al. (2004). Abbreviations of proxies as in Table 1. Y-axes are for original data only. We do not show axes for the filtered signals to avoid unambiguity. Background color is red for interglacials and blue for glacials. Numbers of MIS stages are indicated above the abscissa at the figure bottom. Tie points for tuning of the downhole logging data are given in the Supplement Material 06. (For interpretation of the references to color in this figure legend, the reader is referred to the Web version of this article.)

examining the correlation coefficients, the fact that low variability is present in glacials needs to be considered. Generally, signals from glacials, where we usually see a lower correlation, drag down the overall correlation values. However, even if these values are generally low, they are of statistical relevance (p-value is constantly <0.01). This is also confirmed for the shorter records: Loess from Dolní Věstonice (126–22 ka), $\delta^{18}O$ from Greenland ice (120–0 ka), and TOC from the Lake Van record (264–1 ka; see Table 1 for details).

The records from the south (TOC from Lake Van, wet-dry index from ODP site 967) tend to have higher correlation values (Fig. 5) than those from the north ($\delta^{18}O$ and synthetic records from Greenland). In between are the records from the Iberian Margin, from the Tenaghi Philippon in Greece and most of the records from Lake Ohrid. The correlation coefficients of the different proxies from Lake Ohrid show a wide spread. The maximum value is 0.26 for one of the pollen records (Q.dec; which is at the same time the highest value of all long term (>1 Ma) records). The lowest correlation coefficient of 0.17 is reached in the TIC record (here we have to consider the effect of "low-variability in glacials" described above). The average value for all records of Lake Ohrid results in a correlation coefficient of 0.20 ± 0.03.

The highest correlation (Lake Van, TOC) occurs in a relatively short and young record. This is (at least partly) due to the effect of older parts of the long records generally showing little relation between the original record (black lines in Fig. 4) and the filtered signal (thin red lines in Fig. 4), which lowers their mean correlation coefficient values. To test this variability over time, we determine the correlation coefficients for the time range from 621 ka until recent and for the range from 243 ka until recent. The trend of low values in the north and higher values in the south persists, but the overall correlation coefficients are higher, the younger the time interval. For details see Supplement Material 07.

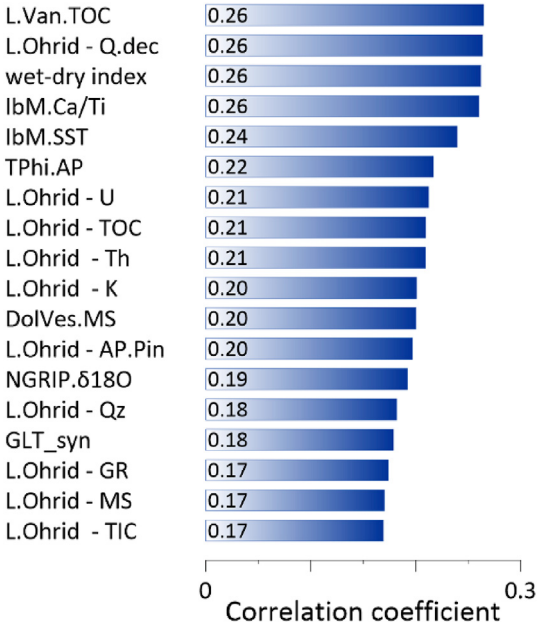

Fig. 5. Correlation coefficients between the original record (black line in Fig. 4) and the bandpassed signal (thin red line in Fig. 4). This table includes all of the investigated data of this study. It has to be taken into account, that three records are significantly shorter (DolVes.MS = 126–22 ka), NGRIP.δ18O = 120–0 ka), and L.Van.TOC = 264–1 ka). All other records cover more than 800 ka. Note that all correlations are significant at >99% confidence. (For interpretation of the references to color in this figure legend, the reader is referred to the Web version of this article.)

3.3. Moving window correlation

Further investigations on the time dependency of the correlation coefficients are possible using the moving window correlation as by Sageman et al. (1999); see chapter 2. 'Material and Methods'. Fig. 6 shows the temporal development of correlation coefficients between original data and the filtered signal (black and thin red line in Fig. 4) of selected proxy records. Overall, the values vary between ~0–0.6 with negligible exceptions of negative correlation (e.g., IbM.Ca/Ti at 232 ka or Q.dec between 885 ka and 845 ka, Fig. 6g and d).

Correlation coefficients are generally higher in the younger part of the records (Fig. 6). Linear fits through the respective running correlation coefficients illustrate this increase. The clarity of the HP signal increases towards the younger parts. The only exception is the record from Lake Van, which is too short for statements about the long-term evolution of the coefficients (Fig. 6f). Despite this divergence of the Lake Van data to the other records, it follows a trend described in the subsequent paragraph.

To some extent, the moving window correlations follow the 405-ka-eccentricity cycle (E_{405}). Although it may be overprinted by effects of the glacial-interglacial variability, we see several similarities between the E_{405} and the pattern of correlation coefficients (Fig. 6) which are high between 600 and 500 ka, and around 200 ka. A good contrary example is MIS 11 where the minimum in E_{405} coincides with minima in correlation coefficients in all shown records. The maximum of E_{405} around MIS 8–6 is reflected in the correlation coefficients of most proxies. Even in glacials, high values in the correlation coefficients are reached (e.g., MIS 8 in the records from Lake Ohrid or MIS 6 in the wet-dry-index from ODP 967 and the Ca/Ti record from the Iberian Margin; Fig. 6a, e and 6g). To some extent this is also true for the older E_{405} maximum (see maximum in MIS 15–13 in GR or Q.dec; Fig. 6a and d), but a clear response is not apparent in this part of the records.

We see a stronger connection of HP to the long-term eccentricity during the last ~621 ka, therefore we focus on this time interval for further investigations on the ~100-ka-eccentricity cycle (E_{100}). We correlate eccentricity to the smoothed envelope derived from the HP signal (purple lines in Fig. 4). The crossplots in Fig. 7 show a wide range of correlation coefficients (r from 0 to 0.74). We notice that the correlation values are highest for the parameters measured on the sediment core of Lake Ohrid (Fig. 7c and d). For most other proxies a clear relationship, and thus the role of E_{100} onto HP, is ambiguous. As described in chapter 2.2 'Time series analysis', we use low-pass filter to assess eccentricity components of the HP amplitude. While a specific eccentricity filter may give clearer results, the applied approach tests if the long term components of the HP amplitude match eccentricity, or if these are influenced by other effects. It should be noted that low correlations do not necessarily mean that there is no relationship between E_{100} and the smoothed HP envelopes. A delayed response of the HP signal to E_{100} is not traceable with this method. For instance, the R-value in the Ca/Ti dataset is 0 (Fig. 7g). Nevertheless, in Fig. 4g we see that the HP envelope (purple line) and the eccentricity (Fig. 4i) are nearly parallel during the last ~500 ka. A systematic offset of ~20 ka is enough to cause this decrease of the correlation value.

We also examined the records for a correlation between obliquity and the envelope of the HP signal (thick red lines and obliquity in Fig. 4. An unambiguous correlation could not be found for any record (see Supplement Material 08).

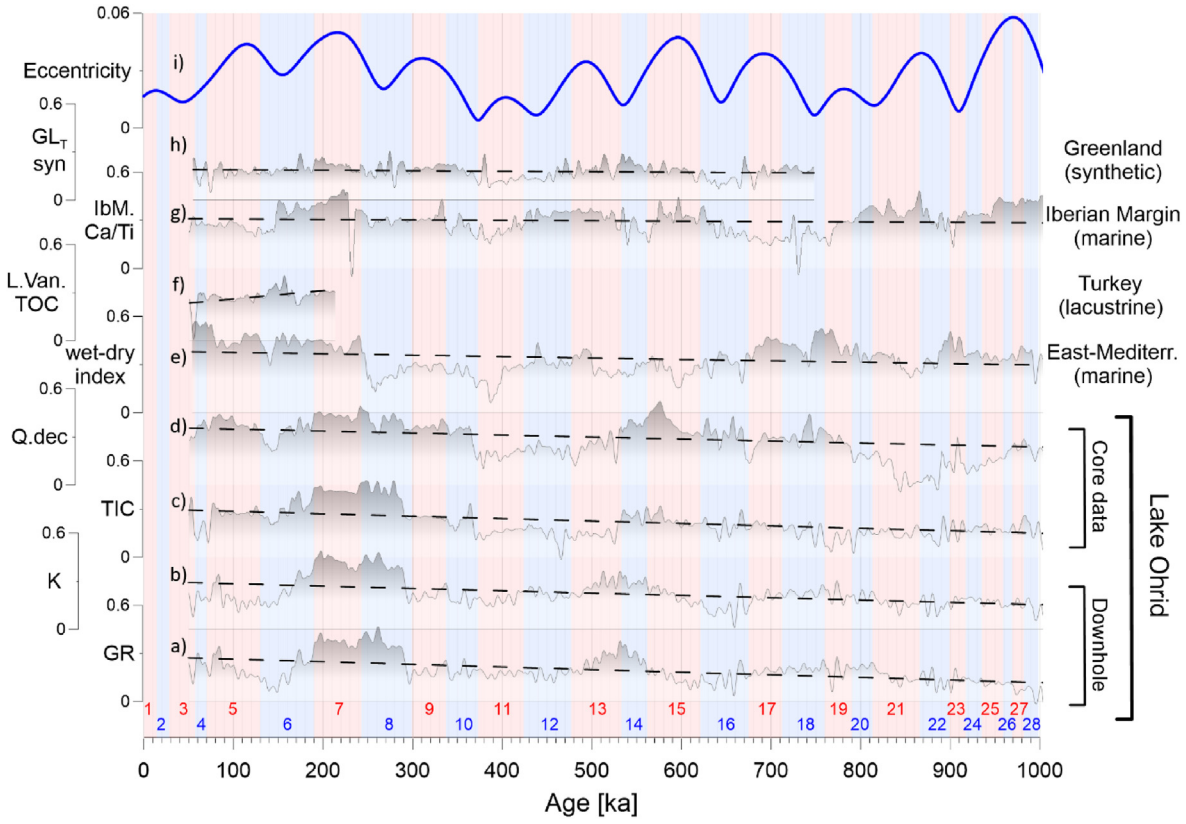

Fig. 6. Relation of correlation coefficients between the original records (black lines in Fig. 4) and the filtered signals (thin red lines in Fig. 4) over time using moving window correlation and trends thereof. Shaded areas indicate periods of high correlation. Details about proxies are listed in Table 1. Dashed lines are linear fits and increase towards the recent (except Lake Van). Marine isotope stages are indicated in red (interglacials) and blue (glacials) numbers. (For interpretation of the references to color in this figure legend, the reader is referred to the Web version of this article.)

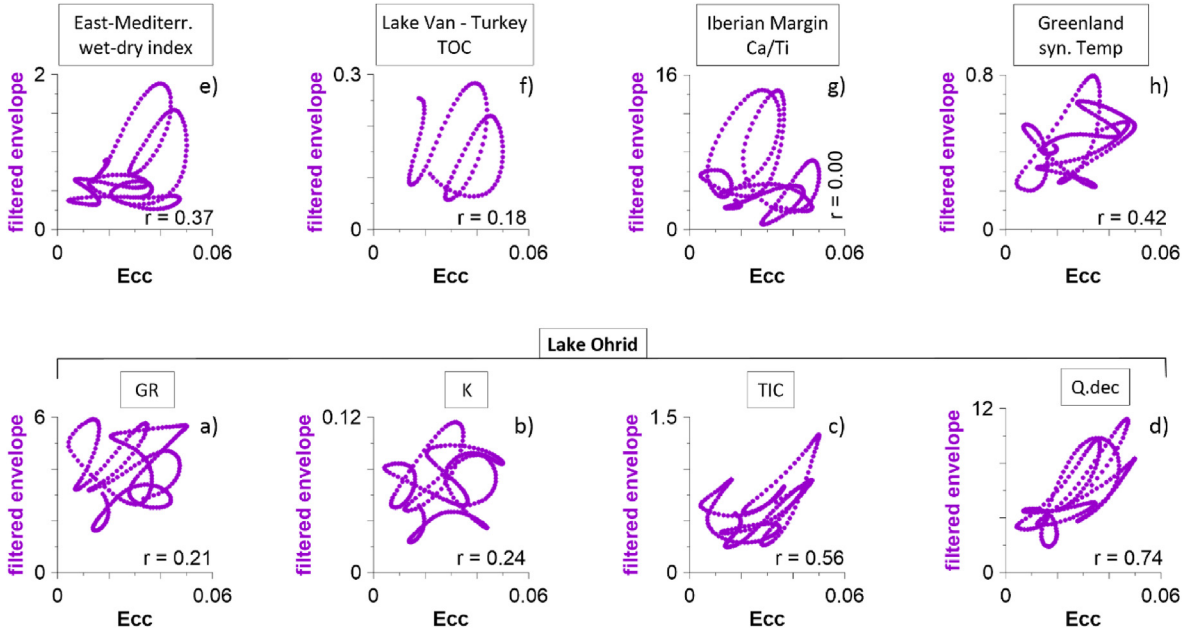

Fig. 7. Crossplots of the filtered envelope (purple line in Fig. 4) to eccentricity (Ecc.). For these plots, only the interval <621 ka (younger than MIS 16) is considered. We observe from Fig. 4 that the relationship of eccentricity to the envelope is ambiguous in parts >621 ka. Coefficients 'r' from Pearson correlation are in the lower right corner. (For interpretation of the references to color in this figure legend, the reader is referred to the Web version of this article.)

4. Discussion

4.1. Detection of the half-precession signal

We use several different methods to characterize the HP signal and its intensity through time. In this regard, all methods have their advantages and challenges, and it is also necessary to consider the different properties of the records.

Power/amplitude spectra are a common tool in cyclostratigraphy. In case orbital cycles are prominently present in a record, they can be recognized rapidly and clearly (Fig. 2; Supplement Material 03). However, amplitude spectra usually represent the complete record and thus also parts where HP is weak and/or superimposed by other frequencies. For this reason, it is possible to get the impression of there being no HP in a record, even though the HP signal is significant in certain time intervals (Supplement Material 04).

Wavelet analysis is an effective method in cyclostratigraphy to assess the variation of signal intensity through depth or time. We can observe the evolution of the HP throughout a record and provide evidence for the occurrence of HP at certain intervals (Fig. 3; Supplement Material 05). An example is the TIC content in Lake Ohrid, where HP is mostly linked to interglacials (Fig. 3c). Wavelet analysis is challenging to interpret when other frequencies superimpose the HP, especially in records with a prominent contribution of high-frequency signals. The synthetic temperature record from Greenland is an example for this feature (Fig. 3h). Overall, this method is suitable for characterizing the occurrence of HP at specific intervals within a record, but straightforward quantification and comparison between different records is challenging.

Therefore, we apply an approach with correlation between original data and filtered data (see chapter 2.2 'Time series analysis'). With this method we can examine a complete record or certain parts of it and obtain one correlation coefficient value for each record (or parts of it). This facilitates comparison with records from other regions (Fig. 5; Supplement Material 07). The moving window correlation after Sageman and Hollander (1999) enables (like the wavelet analysis) the characterization of the HP signal over time. The size of the window should be selected properly; a small window leads to high fluctuations of the correlation coefficients over time, a too large one can lead to smoothing of the coefficients over a longer period of time.

4.2. Characteristics of half-precession in paleoenvironmental records

In many climate records, interglacials have a complex structure with multiple peaks and troughs in proxy values representing variable climate conditions (e.g. Lang and Wolff, 2011; Railsback et al., 2015). An example is the LR04 stack of marine benthic oxygen isotopes (Lisiecki and Raymo, 2005), where several interglacials are separated into substages (e.g. MIS 7a-e, MIS 5a-e). Albeit in these particular cases the subdivision is strongly related to precession, this example shows that proxy signal variations tend to be stronger in interglacials compared to glacials. Similar observations have been made in a lacustrine record from Lake Baikal, where interglacials can be interrupted by short cold periods (Prokopenko et al., 2006). Any proxy should be evaluated individually for its suitability to assess HP signals. Most proxies record the HP signal more accurately in interglacials, but we can distinguish them from proxies that are also capable to record HP in glacials. Even if we group these proxies, the transitions between these groups are smooth.

4.2.1. Interglacial-sensitive proxies

In general, the HP signal in all records examined in this study is more pronounced in interglacials than in glacials. However, there are some cases where the difference between the quality of HP in interglacials is particulary increased compared to glacials.

In our study, the most exceptional case of interglacial sensitivity is the TIC-content in Lake Ohrid (Figs. 3c and 4c). TIC is highly climate sensitive and reflects hydrologic variability. Its amount in Lake Ohrid's sediments is influenced by various factors such as authigenic formation of calcite in the sediments, as well karst runoff triggered by warm conditions (Francke et al., 2016; Wagner et al., 2010, 2019; Vogel et al., 2010).

Also pollen records commonly display the feature of low-variability in glacials, even if not as pronounced as in TIC (e.g. Fig. 4d). This is because certain plant species are completely absent in strong glacials (Wagner et al., 2019; Sadori et al., 2016; Tzedakis et al., 2006).

4.2.2. Proxies capable of recording HP in glacials

The low-variability in glacials is a general property within many climate sensitive proxies, and may complicate analyses of HP. To address this feature, it is necessary to use proxies that are related to amplitude variations also during glacial conditions. In context of Lake Ohrid, this is especially valid for the relative amount of quartz (Qz in Supplement Material 01) and K-concentrations (Fig. 4b). Both are indicators of detrital input (Wagner et al., 2019; Francke et al., 2016).

The wet-dry index introduced by Grant et al. (2017) is based on a sapropel/monsoon index and a dust record (Larrasoaña et al., 2003). This approach is advantageous because the record shows amplitude variations in warm and cold periods, while the variability of other records tend to not encompass both glacials and interglacials equally. Since the index is sensitive to monsoon runoff, it has a stronger connection to low latitude regions than the other examined records.

Hodell et al. (2013) described sub-Milanković cycles in a power spectrum as harmonics of the precession cycle in the Ca/Ti record. However, their study did not focus further on periods shorter than precession. Our focus on the bandwidth between 1/13–1/8.5 facilitates a more detailed investigation of HP in the Ca/Ti record.

4.3. Temporal occurrence of half-precession

The time scale quality of a record can have a relevant impact on the detectability of HP cycles. When time scales are not accurate, HP cycles may appear longer or shorter, and fall out of our filter window. We assume that the used age datasets are robust and that uncertainties in the age-depth calculations do notaffect our overall results. In addition, we address this issue setting the Taner bandpass filters from 8.5 to 13 ka, allowing for imperfect time scales with some distortion, and longer than the actual length of HP cycles (9.5–11.5 ka; Berger et al., 1997). This ensures that the HP signal is detected despite small errors in the time scales.

We observe that the HP signal is generally stronger in interglacials than in glacials. This may be due to the different responses of the proxies to environmental changes, and not an actual weakening of the HP signal in glacial periods (see chapter 4.2 Characteristics of half-precession in paleoenvironmental records'), or an increased HP influence on climate systems during interglacials. HP cycles are very distinctive in some interglacial records. Examples are MIS 7 and MIS 13 in most records of Lake Ohrid (Fig. 4a, b and 4c; Supplement Material 04), MIS 5 of the wet-dry index from the Eastern Mediterranean (Fig. 4e) and pollen from Lake Ohrid (Fig. 4d). However, depending on the selection of a proxy and its sensitivity to environmental changes, we occasionally

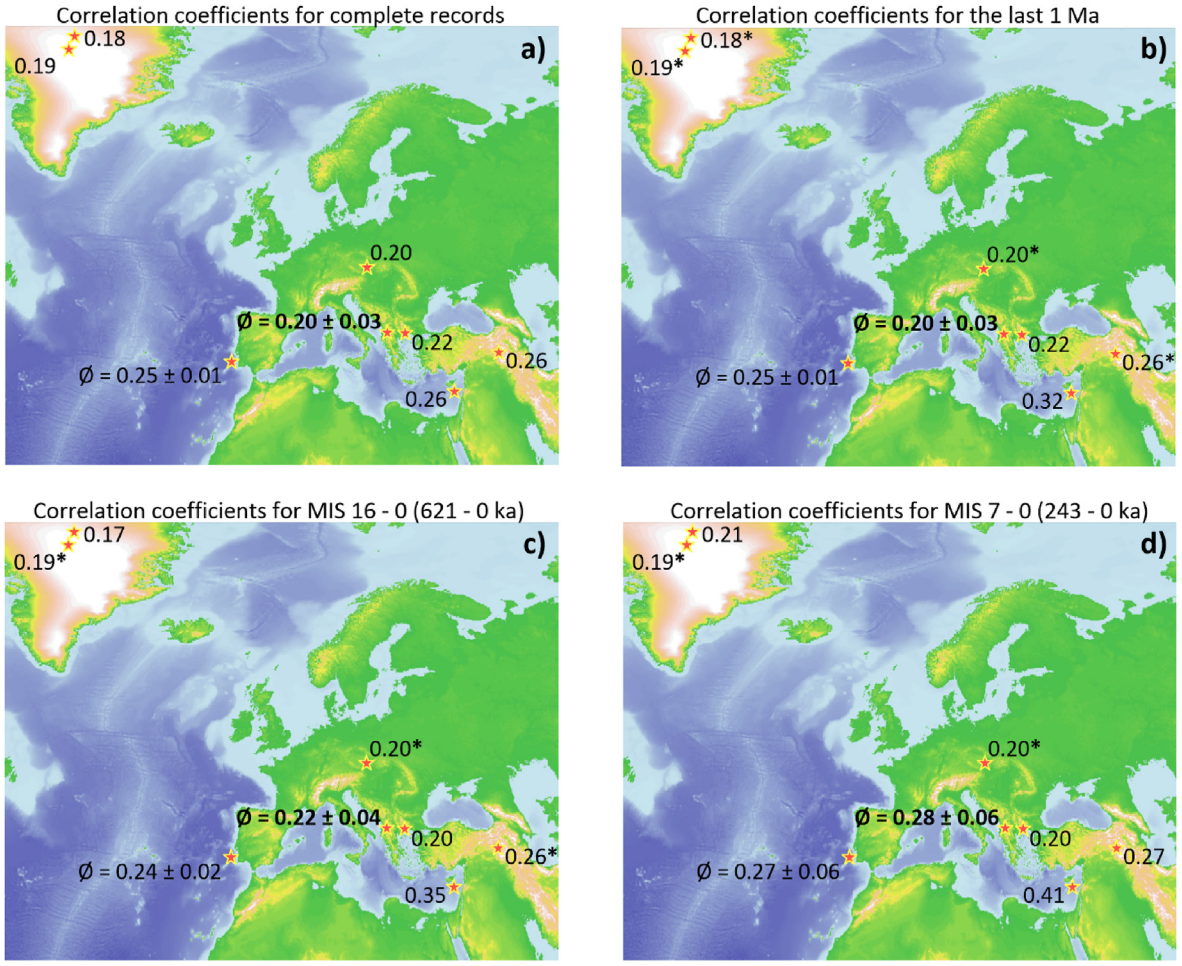

Fig. 8. Correlation coefficients as proxy for the relative contribution and clarity of the HP signal at the investigated sites in different time intervals (a–d). Lake Ohrid data is bold. Values marked with asterisks (*) are from data sets that are shorter than the time interval specified in the respective title (see Table 1 for exact time span of individual records). Average values (Ø) and standard deviations are from sites where multiple datasets are available (two records from the Iberian Margin and ten from Lake Ohrid). Note that the correlation values generally increase towards the younger intervals (from a-d; as the linear trends in Fig. 6).

recognize HP in glacials. Examples are MIS 12 in the Ca/Ti from the Iberian Margin (Fig. 4g) or MIS 16 and MIS 12 in the wet-dry index from the Eastern Mediterranean (Fig. 4e).

In addition to the variability of the HP signal between interglacials and glacials, we see a consistent trend of increasing HP signal towards the recent (Fig. 6). A possible explanation for this trend is the change from the 40-ka to the 100-ka world during the Mid-Pleistocene Transition (MPT; Shackleton and Opdyke, 1976). Since precession is modulated by eccentricity, a similar effect may be expected for the HP signal. This idea is supported by the presence of a positive correlation between HP and eccentricity (Figs. 6 and 7) in the younger part (<621 ka) of the investigated records, but the absence of such a relation between HP and obliquity (Supplement Material 08).

If assuming a relation of HP to eccentricity, one may expect a weaker expression of HP in an obliquity dominated world. Such conditions prevailed before and partly during the MPT ~1.25 to 0.7 million years ago (Pisias and Moore, 1981; Clark et al., 2006; Mudelsee and Schulz, 1997). The length of most examined records in this study does not allow assessment of HP before MPT. In the records from Lake Ohrid, the MPT is partly covered and we see an increase of HP intensity during and after the MPT. After MIS 16, the HP signal is more prominent and follows partly the E_{405} cycle while before MIS 16 (in the younger part of the MPT) the clarity of the HP signal vanishes (Fig. 6). Therefore, the HP signal in Lake Ohrid appears to be not only affected by glacial or interglacial conditions, but also by orbital eccentricity and specifically the E_{405} cycle.

4.4. Spatial occurrence of half-precession around Europe

The correlation coefficients between the paleoclimate proxy datasets and HP filters listed in Fig. 5 are an indicator of the clarity of HP signal in each record. Fig. 8a shows those values on a map of Europe and the North Atlantic. In shorter and younger time intervals, this relation persists and the gradient between the regions even increases (Fig. 8a–d and Fig. 9a–d). The r-values in Greenland remain almost equally low while values in the Eastern Mediterranean increase clearly from 0.26 to 0.41. The records from the Iberian Margin and Lake Ohrid (which are - from a spatial point of view - between the Eastern Mediterranean and Greenland), show intermediate changes in the clarity of the HP signal over time. Thus, we observe a trend of stronger HP signal in data from the southeast to weaker HP signal in the northwest. Fig. 9 illustrates this relationship with respect to latitude for four time intervals. The pattern of higher correlation coefficients in the south - and thus higher clarity of HP - is even stronger in the younger part of the records (Fig. 9d).

In Figs. 8 and 9, we use an average r-value for all sites with multiple datasets (two datasets on the Iberian Margin, ten datasets

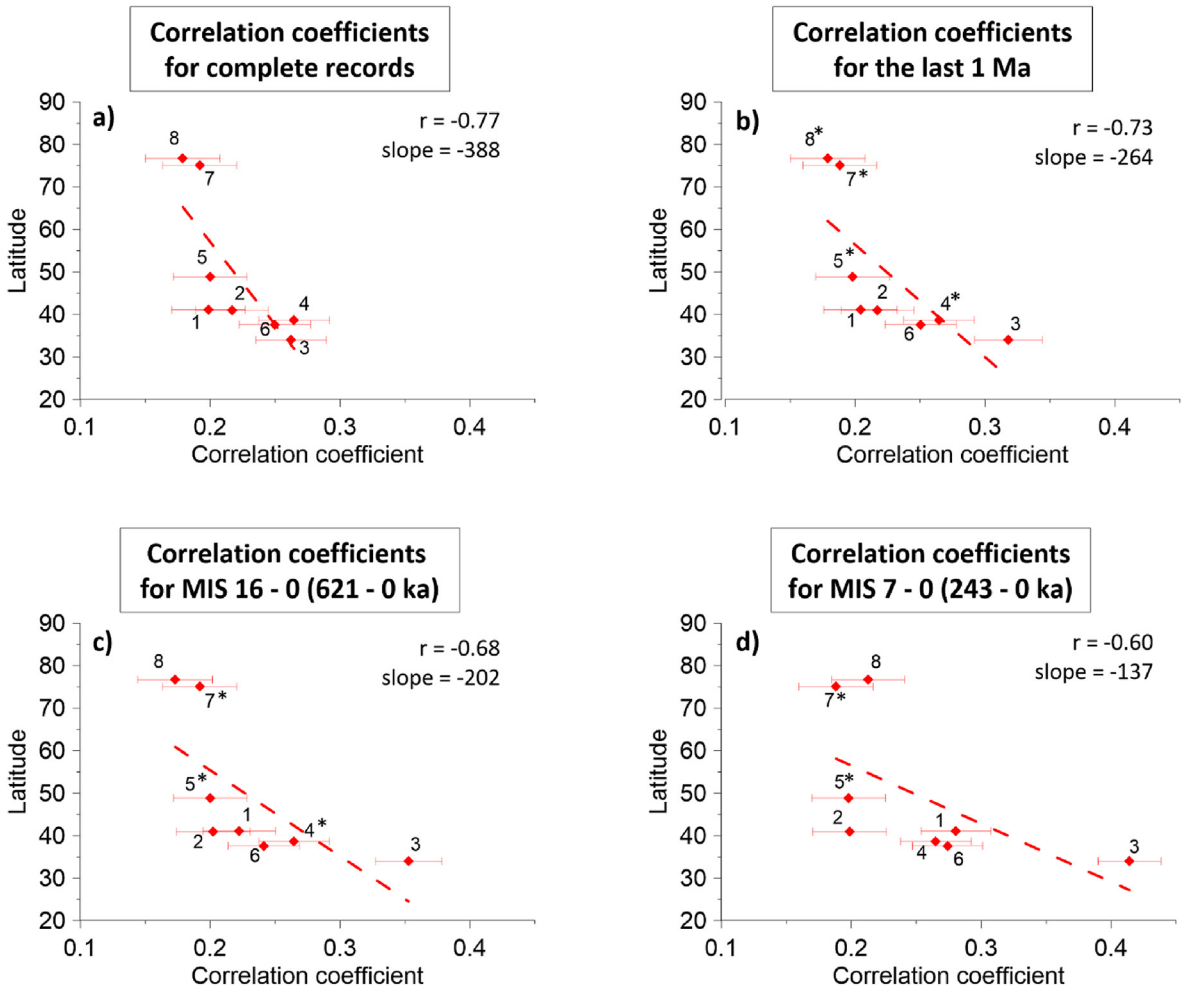

Fig. 9. Correlation coefficients between original data (black lines in Fig. 4) and bandpassed signals (thin red line in Fig. 4) as proxy for the clarity of HP cycles against latitude for the investigated sites. Time intervals as in Fig. 8. Uncertainty estimated as explained in Supplement Material 09. We use the average standard deviation for sites where multiple datasets are available (two records from the Iberian Margin and ten from Lake Ohrid). Dashed line is a linear fit with slope values given in each subplot (a–d). The relationship between latitude and clarity of HP (here correlation) is changing through time. The difference in HP clarity between the Mediterranean region and Greenland is increasing through time from a) longest time interval to d) youngest interval. Also note that data marked with asterisks (*) are from records that are shorter than the time interval specified in the respective title (see Table 1 for exact time span of individual records). 1. Lake Ohrid, Albania/North Macedonia; 2. Tenaghi Philippon, Greece; 3. ODP Site 967, Eastern Mediterranean; 4. Lake Van, Turkey; 5. Dolní Věstonice, Czech Republic; 6. IODP Site U1385 "Shackleton site", Iberian Margin; 7. NGRIP, Greenland; 8. Synthetic record, Greenland (see Table 1 for proxy details and Fig. 1 for location on the map). (For interpretation of the references to color in this figure legend, the reader is referred to the Web version of this article.)

in Lake Ohrid). Especially in records from Lake Ohrid, the range in r from 0.17 to 0.26 is relatively wide (Fig. 5). Despite this range we see an increase of average values towards the recent (Fig. 9).

Several studies demonstrated HP cycles in low latitude records (e.g. Hagelberg et al., 1994; Trauth et al., 2003). The HP signal is expected to be strongest in equatorial regions where the twice-yearly passage of the sun over the equator creates a precession harmonic at 10–12 cycles/ka (Hagelberg et al., 1994; Short et al., 1991). HP from a lacustrine record in East Africa illustrates the connection of HP cyclicity to the monsoonal system (Verschuren et al., 2009). The previous findings that HP is a mainly tropical signal is in agreement with our investigations. The closer a record is to the influence area of a monsoon system, the stronger is the HP signal. In our study, this is most evident in the ODP 967 (Grant et al., 2017) and Lake Ohrid records (Wagner et al., 2019). Towards higher latitudes the HP signal decreases gradually, but weak signals are still found in records from Greenland. High and low latitudes in the North Atlantic appear decoupled prior to the initiation of Northern Hemisphere glaciation, but strongly coupled thereafter (deMenocal et al., 1993; Hagelberg et al., 1994).

When comparing different data from different regions, several aspects like the catchment areas or regional environmental changes need to be considered. As an example, we examine the records from Lake Ohrid and the ODP 967 core from the eastern Mediterranean (Grant et al., 2017). Although both are basically a two component system (Lake Ohrid: non calcareous clay/calcareous clay (Francke et al., 2016); ODP 967: detrital input/sapropels (Grant et al., 2017), they differ by the extent of their catchment area. Local geological influences like tectonic movement in the catchment area of Lake Ohrid may affect the recording of climate signals. In comparison, the ODP core with its catchment of large parts of Africa will not be as sensitive to such small-scale events. However, in lake environments we often observe high sedimentation rates and thus, a good temporal resolution, which in turn is advantageous for the preservation of (Sub-)Milanković cycles. The same holds for terrestrial records like the loess record from Czech Republic (Supplement Material 01; Antoine et al., 2013; Fuchs et al., 2013). Due to better resolution, the HP signal is preserved very well in certain short time intervals (e.g. early MIS 5), but such records cover only a short time interval (e.g., 126–22 ka). Marine

records are often more constant regarding preservation of changes in environmental conditions over long time periods, but often have lower sedimentation rates. All of this needs to be considered when analyzing records in terms of short orbital cycles (and other high-frequency signals). Not only the type of proxy is relevant for the preservation of HP, but also the regional environmental conditions of the location from which the record originates.

4.5. Implications for the origin of half-precession in the studied region

Until now HP is poorly understood and only described in single records. Heinrich (1988) demonstrated the existence of an 11 ± 1 ka cycle based on the occurrence of ice rafted debris in marine sediments of the North Atlantic, as increased ice runoff occurred during solar radiation maxima/minima. Also Hinnov et al. (2002) proved the occurrence of HP in high latitudes and suggested a link to Dansgaard-Oeschger events. On the other hand, there are considerably more studies describing the origin of HP in equatorial regions as a result of the two insolation maxima per precession cycle (e.g. Berger et al., 1997; Laepple and Lohmann, 2009; Trauth et al., 2003). Here, we analyze HP in a suite of records in order to better understand its spatial occurrence allowing to discuss its climatic origin.

We observe a clear gradient in the intensity of HP in European and North Atlantic regions. The signal is clearest in the southeast, and may be influenced by the Asian and/or African monsoonal systems. However, the HP signal (even if significantly weaker) in the high latitudes like Greenland cannot be directly affected by the low latitude monsoon systems. Sun and Huang (2006) and also Turney et al. (2004) demonstrated that information about HP can be transferred from low to high latitudes. We suggest that when information (about HP) propagates via atmospheric and/or oceanic teleconnections, more of the information dissipates as the distance from the source of the HP signal increases. Additionally, other (orbital) signals may overprint the HP signal in high latitudes (e.g. Short et al., 1991; Hodell et al., 2013).

Alternatively, the HP signal in high latitudes may have a different mechanistic origin from the HP in low latitudes. In low latitudes the HP is a predominantly interglacial feature, possibly because the high precession amplitude during high eccentricity transports signals from one hemisphere over the equator to the other hemisphere. Contrary, in Greenland HP occurs regardless of variability between glacials and interglacials, albeit at comparably weak levels.

In Figs. 8 and 9, we demonstrate that the clarity of HP signal is stronger in the southern records and is generally increasing towards the recent. Our results suggest that the HP signal originates in the south and that this pattern is partially transported to high latitudes. We illustrate that despite a pronounced increase of the HP in the south, it is only weakly transported to the high latitudes of the Greenland records.

Assuming that the main source of the HP signal is in equatorial regions and that HP signals in high-latitude records must be transmitted from there, we see the potential of HP as an indicator for the connectivity between low- and high-latitude climate systems over time, at least in the European/North Atlantic region.

In this context our analysis shows strongest HP and connectivity of the Iberian Margin to the tropics during interglacials and especially in the high-eccentricity (high precession amplitude) interval of MIS 7 (Fig. 6). Contrary, little HP is transmitted to the Mediterranean region during the glacials, though the strongest HP signals occur in the eastern Mediterranean, where the signal is carried via the Nile River.

Kaboth-Bahr et al. (2018) suggest that the monsoonal influence on the water density structure in the Mediterranean affects the variability of the Mediterranean Outflow Water (MOW), which effectively transmits a low-latitude orbital pacing to the East Atlantic off Iberia and via atmospheric moisture transport to the European continent. In the late Quaternary, low precession amplitudes led to less severe dry phases in North Africa and thus less prominent peaks in MOW strength. If we consider the MOW as a transport mechanism for the HP signal, this is in agreement with the low HP signature in the low precession amplitude phases during MIS 14 and 11 in the Iberian Margin record (Fig. 6g). In contrast there was a phase with high MOW production caused by particularly pronounced aridity phases during MIS 6 within the E_{400}-maximum (Kaboth-Bahr et al., 2018; Trauth et al., 2009). Again, we can see a connection of the HP records from the Mediterranean to the Iberian Margin as the increased MOW probably transferred the HP signal during MIS 6 (Fig. 6e and g). This implies an astronomically forced shift of climate systems over the Mediterranean region. One prominent driver is the Nile discharge, which modulates the Mediterranean circulation and even influences the outflow of the Mediterranean Sea into the Atlantic Ocean.

5. Conclusions

The good temporal resolution and the continuity of the records in Lake Ohrid provide excellent prerequisites for cyclostratigraphic studies. In a suite of sedimentary proxies, there is recurrent evidence of HP cycles from the Mid-Pleistocene to the recent. The expression of HP cycles is generally stronger in the younger parts of the data (<MIS 16) and during interglacials. The latter may partly result from the natural behavior of proxies.

In several records from Lake Ohrid, a relationship between HP and eccentricity cycles exists. Even a connection to the long term 405-ka-eccentricity cycle is apparent after the Mid-Pleistocene Transition. However, a correlation between the HP envelope and obliquity is absent. We interpret this as a relation of HP and precession and its amplitude.

HP is present in all examined datasets between Greenland and the Eastern Mediterranean, although the proxies are dominated by different climate systems. The reasons for the appearance of the HP signal in different records may be diverse, but we see a distinct trend from weaker HP signals in the North Atlantic to a stronger signature in the Eastern Mediterranean region. The clarity of the HP signal between the Atlantic and the Mediterranean appears to be gradual, as are the transitions between the causative climate systems. We suggest that the equatorial HP signal is transported northward via different modes. Besides Nile water discharge and Mediterranean Outflow Water, the connected Monsoon systems are one major driver in this process. The sediment succession from Lake Ohrid appears to be a link between the high and low latitudes climate systems; Wagner et al. (2019) describe a connection to the African monsoon. We identify a similar influence of low latitudes on Lake Ohrid expressed as the distinctness of the HP signal in the records.

HP is a relevant part of natural climate variability - also in Europe especially in interglacials. Its probable origin in low latitudes and the possible transmission of the HP signal to high latitudes gives HP the potential to be an indicator for the interconnectivity of paleoclimate systems.

Author contribution

Zeeden, Christian Scientific support during study design. Discussion, especially for time series analysis. Writing/editing the manuscript. Prof. Dr. Voigt, Silke Scientific support and discussion, especially for spatial context of the half-precession signal. Writing/

editing the manuscript. Dr. Sardar Abadi, Mehrdad Scientific support and discussion. Writing/editing the manuscript. Dr. Wonik, Thomas Scientific support and discussion, especially in downhole logging data acquisition and interpretation.

Declaration of competing interest

The authors declare that they have no known competing financial interests or personal relationships that could have appeared to influence the work reported in this paper.

Acknowledgements

This research project was possible due to funding from the German Research Foundation (grant WO672/15). The “Scientific Collaboration on Past Speciation Conditions in Lake Ohrid” (SCOPSCO) drilling project was partly funded by grants from the International Continental Scientific Drilling Program (ICDP), the German Ministry of Higher Education and Research, the German Research Foundation, the University of Cologne, the British Geological Survey, the Italian National Institute of Geophysics and Volcanology (INGV) and the Italian National Research Council (CNR) and the governments of the republics of North Macedonia (or FYROM) and Albania. We would like to thank the whole SCOPSCO team for helpful discussions about the results. The boreholes were drilled by Drilling, Observation and Sampling of the Earth's Continental Crust, Inc. Our special thanks go to Thomas Grelle, Jan-Thorsten Blanke and Dr. Henrike Baumgarten of the Leibniz Institute for Applied Geophysics for the acquisition of the geophysical downhole logging data. We also appreciate the work of anonymous reviewers and editors.

Appendix A. Supplementary data

Supplementary data to this article can be found online at https://doi.org/10.1016/j.quascirev.2022.107413.

References

Amante, C., Eakins, B.W., 2009. ETOPO1 Arc-Minute Global Relief Model: Procedures, Data Sources and Analysis.

Antoine, P., Rousseau, D.-D., Degeai, J.-P., Moine, O., Lagroix, F., kreutzer, S., Fuchs, M., Hatté, C., Gauthier, C., Svoboda, J., Lisá, L., 2013. High-resolution record of the environmental response to climatic variations during the Last Interglacial–Glacial cycle in Central Europe: the loess-palaeosol sequence of Dolní Věstonice (Czech Republic). Quat. Sci. Rev. 67, 17–38. https://doi.org/10.1016/j.quascirev.2013.01.014.

Barker, S., Knorr, G., Edwards, R.L., Parrenin, F., Putnam, A.E., Skinner, L.C., Wolff, E., Ziegler, M., 2011. 800,000 Years of abrupt climate variability. Science 334, 347–351. https://doi.org/10.1126/science.1203580.

Baumgarten, H., Wonik, T., Tanner, D.C., Francke, A., Wagner, B., Zanchetta, G., Sulpizio, R., Giaccio, B., Nomade, S., 2015. Age–depth model of the past 630 kyr for Lake Ohrid (FYROM/Albania) based on cyclostratigraphic analysis of downhole gamma ray data. Biogeosciences 12, 7453–7465. https://doi.org/10.5194/bg-12-7453-2015.

Berger, A., Loutre, M.F., McIntyre, A., 1997. Intertropical latitudes and precessional and half-precessional cycles. Science 278, 1476–1478.

Berger, A., Loutre, M.F., Mélice, J.L., 2006. Equatorial insolation: from precession harmonics to eccentricity frequencies. Clim. Past 2, 131–136. https://doi.org/10.5194/cp-2-131-2006.

Broecker, W.S., 1998. Paleocean circulation during the Last Deglaciation: a bipolar seesaw? Paleoceanography 13, 119–121. https://doi.org/10.1029/97PA03707.

Clark, P.U., Archer, D., Pollard, D., Blum, J.D., Rial, J.A., Brovkin, V., Mix, A.C., Pisias, N.G., Roy, M., 2006. The middle Pleistocene transition: characteristics, mechanisms, and implications for long-term changes in atmospheric pCO2. Quat. Sci. Rev., Critical Quaternary Stratigraphy 25, 3150–3184. https://doi.org/10.1016/j.quascirev.2006.07.008.

Colcord, D.E., Shilling, A.M., Sauer, P.E., Freeman, K.H., Njau, J.K., Stanistreet, I.G., Stollhofen, H., Schick, K.D., Toth, N., Brassell, S.C., 2018. Sub-Milankovitch paleoclimatic and paleoenvironmental variability in East Africa recorded by Pleistocene lacustrine sediments from Olduvai Gorge, Tanzania. Palaeogeogr. Palaeoclimatol. Palaeoecol. 495, 284–291. https://doi.org/10.1016/j.palaeo.2018.01.023.

De Vleeschouwer, D., Da Silva, A.C., Boulvain, F., Crucifix, M., Claeys, P., 2012. Precessional and half-precessional climate forcing of Mid-Devonian monsoon-like dynamics. Clim. Past 8, 337–351. https://doi.org/10.5194/cp-8-337-2012.

deMenocal, P.B., Ruddiman, W.F., Pokras, E.M., 1993. Influences of high- and low-latitude processes on african terrestrial climate: Pleistocene Eolian records from equatorial Atlantic Ocean drilling Program site 663. Paleoceanography 8, 209–242. https://doi.org/10.1029/93PA02688.

Francke, A., Wagner, B., Just, J., Leicher, N., Gromig, R., Baumgarten, H., Vogel, H., Lacey, J.H., Sadori, L., Wonik, T., Leng, M.J., Zanchetta, G., Sulpizio, R., Giaccio, B., 2016. Sedimentological processes and environmental variability at Lake Ohrid (Macedonia, Albania) between 637 ka and the present. Biogeosciences 13, 1179–1196. https://doi.org/10.5194/bg-13-1179-2016.

Fuchs, M., Kreutzer, S., Rousseau, D.-D., Antoine, P., Hatté, C., Lagroix, F., Moine, O., Gauthier, C., Svoboda, J., Lisá, L., 2013. The loess sequence of Dolní Věstonice, Czech republic: a new OSL-based chronology of the last climatic cycle. Boreas 42, 664–677. https://doi.org/10.1111/j.1502-3885.2012.00299.x.

Grant, K.M., Rohling, E.J., Westerhold, T., Zabel, M., Heslop, D., Konijnendijk, T., Lourens, L., 2017. A 3 million year index for North African humidity/aridity and the implication of potential pan-African Humid periods. Quat. Sci. Rev. 171, 100–118. https://doi.org/10.1016/j.quascirev.2017.07.005.

Hagelberg, T.K., Bond, G., deMenocal, P., 1994. Milankovitch band forcing of sub-Milankovitch climate variability during the Pleistocene. Paleoceanography 9, 545–558. https://doi.org/10.1029/94PA00443.

Hays, J., Imbrie, J., Shackleton, N., 1976. Variations in the earth's orbit: pacemaker of the ice ages. Science 194, 1121–1132. https://doi.org/10.1126/science.194.4270.1121.

Heinrich, H., 1988. Origin and consequences of cyclic ice rafting in the Northeast Atlantic Ocean during the past 130,000 years. Quat. Res. 29, 142–152. https://doi.org/10.1016/0033-5894(88)90057-9.

Hinnov, L.A., 2000. New perspectives on orbitally forced stratigraphy. Annu. Rev. Earth Planet Sci. 28, 419–475. https://doi.org/10.1146/annurev.earth.28.1.419.

Hinnov, L.A., Schulz, M., Yiou, P., 2002. Interhemispheric space–time attributes of the Dansgaard–Oeschger oscillations between 100 and 0ka. Quat. Sci. Rev., Decadal-to-Millennial-Scale Climate Variability 21, 1213–1228. https://doi.org/10.1016/S0277-3791(01)00140-8.

Hodell, D., Crowhurst, S., Skinner, L., Tzedakis, P.C., Margari, V., Channell, J.E.T., Kamenov, G., Maclachlan, S., Rothwell, G., 2013. Response of Iberian Margin sediments to orbital and suborbital forcing over the past 420 ka. Paleoceanography 28, 185–199. https://doi.org/10.1002/palo.20017.

Hodell, D., Lourens, L., Crowhurst, S., Konijnendijk, T., Tjallingii, R., Jiménez-Espejo, F., Skinner, L., Tzedakis, P.C., Abrantes, F., Acton, G.D., Alvarez Zarikian, C.A., Bahr, A., Balestra, B., Barranco, E.L., Carrara, G., Ducassou, E., Flood, R.D., Flores, J.-A., Furota, S., Grimalt, J., Grunert, P., Hernández-Molina, J., Kim, J.K., Krissek, L.A., Kuroda, J., Li, B., Lofi, J., Margari, V., Martrat, B., Miller, M.D., Nanayama, F., Nishida, N., Richter, C., Rodrigues, T., Rodríguez-Tovar, F.J., Roque, A.C.F., Sanchez Goñi, M.F., Sierro Sánchez, F.J., Singh, A.D., Sloss, C.R., Stow, D.A.V., Takashimizu, Y., Tzanova, A., Voelker, A., Xuan, C., Williams, T., 2015. A reference time scale for site U1385 (Shackleton site) on the SW Iberian margin. Global Planet. Change 133, 49–64. https://doi.org/10.1016/j.gloplacha.2015.07.002.

Hooghiemstra, H., 2006. Leitfaden der Pollenbestimmung Fur Mitteleuropa und angrenzende Gebiete. H.-J. Beug. Publisher Verlag Friedrich Pfeil, Munich, 2004 (542 pp. 120 plates, 12 tables) ISBN 3 89937 043 0. J. Quat. Sci. 21, 105. https://doi.org/10.1002/jqs.915.

Kaboth-Bahr, S., Bahr, A., Zeeden, C., Toucanne, S., Eynaud, F., Jiménez-Espejo, F., Röhl, U., Friedrich, O., Pross, J., Löwemark, L., Lourens, L.J., 2018. Monsoonal forcing of European ice-sheet dynamics during the late quaternary. Geophys. Res. Lett. 45, 7066–7074. https://doi.org/10.1029/2018GL078751.

Kodama, K.P., Hinnov, L.A., 2014. Rock Magnetic Cyclostratigraphy. John Wiley & Sons.

Kutzbach, J.E., Chen, G., Cheng, H., Edwards, R.L., Liu, Z., 2014. Potential role of winter rainfall in explaining increased moisture in the Mediterranean and Middle East during periods of maximum orbitally-forced insolation seasonality. Clim. Dynam. 42, 1079–1095. https://doi.org/10.1007/s00382-013-1692-1.

Laepple, T., Lohmann, G., 2009. Seasonal cycle as template for climate variability on astronomical timescales. Paleoceanography 24. https://doi.org/10.1029/2008PA001674.

Lang, N., Wolff, E.W., 2011. Interglacial and glacial variability from the last 800 ka in marine, ice and terrestrial archives. Clim. Past 7, 361–380. https://doi.org/10.5194/cp-7-361-2011.

Larrasoaña, J.C., Roberts, A.P., Rohling, E.J., Winklhofer, M., Wehausen, R., 2003. Three million years of monsoon variability over the northern Sahara. Clim. Dynam. 21, 689–698. https://doi.org/10.1007/s00382-003-0355-z.

Laskar, J., Robutel, P., Joutel, F., Gastineau, M., Correia, A.C.M., Levrard, B., 2004. A long-term numerical solution for the insolation quantities of the Earth. Astron. Astrophys. 428, 261–285. https://doi.org/10.1051/0004-6361:20041335.

Leicher, N., Zanchetta, G., Sulpizio, R., Giaccio, B., Wagner, B., Nomade, S., Francke, A., Del Carlo, P., 2016. First tephrostratigraphic results of the DEEP site record from Lake Ohrid (Macedonia and Albania). Biogeosciences 13, 2151–2178. https://doi.org/10.5194/bg-13-2151-2016.

Li, M., Huang, C., Ogg, J., Zhang, Y., Hinnov, L., Wu, H., Chen, Z.-Q., Zou, Z., 2019. Paleoclimate proxies for cyclostratigraphy: comparative analysis using a Lower Triassic marine section in South China. Earth-Sci. Rev., Sedimentology as a Key to Understanding Earth and Life Processes 189, 125–146. https://doi.org/10.1016/j.earscirev.2019.01.011.

Liebrand, D., de Bakker, A.T.M., 2019. Bispectra of climate cycles show how ice ages are fuelled. Clim. Past 15, 1959–1983. https://doi.org/10.5194/cp-15-1959-2019.
Lionello, P., Abrantes, F., Congedi, L., Dulac, F., Gacic, M., Gomis, D., Goodess, C., Hoff, H., Kutiel, H., Luterbacher, J., Planton, S., Reale, M., Schröder, K., Struglia, M.V., Toreti, A., Tsimplis, M., Ulbrich, U., Xoplaki, E., 2012. Introduction: mediterranean climate—background information. Clim. Mediterr. Reg. https://doi.org/10.1016/B978-0-12-416042-2.00012-4. Past Future xxxv–xc.
Lisiecki, L.E., Raymo, M.E., 2005. A Pliocene-Pleistocene stack of 57 globally distributed benthic δ18O records. Paleoceanography 20. https://doi.org/10.1029/2004PA001071.
Liu, Y., Liang, X.S., Weisberg, R.H., 2007. Rectification of the Bias in the wavelet power spectrum. J. Atmos. Ocean. Technol. 24, 2093–2102. https://doi.org/10.1175/2007JTECHO511.1.
Meyers, S.R., 2019. Cyclostratigraphy and the problem of astrochronologic testing. Earth Sci. Rev. 190, 190–223. https://doi.org/10.1016/j.earscirev.2018.11.015.
Meyers, S., Malinverno, A., Hinnov, L., Zeeden, C., Liu, H., Moron, V., 2021. astrochron: A Computational Tool for Astrochronology.
Milanković, 1920. Théorie Mathématique des Phénomènes Thermiques Produits par la Radiation Solaire. Acad. Yougosl. Sci. Arts Zagreb.
Milanković, M.K., 1941. Kanon der Erdbestrahlung und seine Anwendung auf das Eiszeitenproblem. R. Serbian Acad. Spec. Publ. 133, 1–633.
Mudelsee, M., Schulz, M., 1997. The Mid-Pleistocene climate transition: onset of 100 ka cycle lags ice volume build-up by 280 ka. Earth Planet Sci. Lett. 151, 117–123. https://doi.org/10.1016/S0012-821X(97)00114-3.
North_Greenland_Ice-Core_Project_members, Andersen, K.K., Azuma, N., Barnola, J.-M., Bigler, M., Biscaye, P., Caillon, N., Chappellaz, J., Clausen, H.B., Dahl-Jensen, D., Fischer, H., Flückiger, J., Fritzsche, D., Fujii, Y., Goto-Azuma, K., Grønvold, K., Gundestrup, N.S., Hansson, M., Huber, C., Hvidberg, C.S., Johnsen, S.J., Jonsell, U., Jouzel, J., Kipfstuhl, S., Landais, A., Leuenberger, M., Lorrain, R., Masson-Delmotte, V., Miller, H., Motoyama, H., Narita, H., Popp, T., Rasmussen, S.O., Raynaud, D., Röthlisberger, R., Ruth, U., Samyn, D., Schwander, J., Shoji, H., Siggard-Andersen, M.-L., Steffensen, J.P., Stocker, T., Sveinbjörnsdottir, A.E., Svensson, A., Takata, M., Tison, J.-L., Thorsteinsson, T., Watanabe, O., Wilhelms, F., White, J., 2004. High-resolution record of the Northern Hemisphere climate extending into the last interglacial period. Nature 431, 147–151.
Pisias, N.G., Moore, T.C., 1981. The evolution of Pleistocene climate: a time series approach. Earth Planet Sci. Lett. 52, 450–458. https://doi.org/10.1016/0012-821X(81)90197-7.
Prokopenko, A.A., Hinnov, L.A., Williams, D.F., Kuzmin, M.I., 2006. Orbital forcing of continental climate during the Pleistocene: a complete astronomically tuned climatic record from Lake Baikal, SE Siberia. Quat. Sci. Rev., Critical Quaternary Stratigraphy 25, 3431–3457. https://doi.org/10.1016/j.quascirev.2006.10.002.
R Core Team, 2021. R: The R Project for Statistical Computing.
Railsback, L.B., Gibbard, P.L., Head, M.J., Voarintsoa, N.R.G., Toucanne, S., 2015. An optimized scheme of lettered marine isotope substages for the last 1.0 million years, and the climatostratigraphic nature of isotope stages and substages. Quat. Sci. Rev. 111, 94–106. https://doi.org/10.1016/j.quascirev.2015.01.012.
Rider, M., Kennedy, M., 2011. The Geological Interpretation of Well Logs. Rider-French.
Rodrigues, T., Alonso-García, M., Hodell, D.A., Rufino, M., Naughton, F., Grimalt, J.O., Voelker, A.H.L., Abrantes, F., 2017. A 1-Ma record of sea surface temperature and extreme cooling events in the North Atlantic: a perspective from the Iberian Margin. Quat. Sci. Rev. 172, 118–130. https://doi.org/10.1016/j.quascirev.2017.07.004.
Rohling, E.J., Marino, G., Grant, K.M., 2015. Mediterranean climate and oceanography, and the periodic development of anoxic events (sapropels). Earth Sci. Rev. 143, 62–97. https://doi.org/10.1016/j.earscirev.2015.01.008.
Rossignol-Strick, M., 1985. Mediterranean Quaternary sapropels, an immediate response of the African monsoon to variation of insolation. Palaeogeogr. Palaeoclimatol. Palaeoecol. 49, 237–263. https://doi.org/10.1016/0031-0182(85)90056-2.
Sadori, L., Koutsodendris, A., Panagiotopoulos, K., Masi, A., Bertini, A., Combourieu-Nebout, N., Francke, A., Kouli, K., Joannin, S., Mercuri, A.M., Peyron, O., Torri, P., Wagner, B., Zanchetta, G., Sinopoli, G., Donders, T.H., 2016. Pollen-based paleoenvironmental and paleoclimatic change at Lake Ohrid (south-eastern Europe) during the past 500 ka. Biogeosciences 13, 1423–1437. https://doi.org/10.5194/bg-13-1423-2016.
Sageman, B.B., Hollander, D.J., 1999. Cross correlation of paleoecological and geochemical proxies: a holistic approach to the study of past global change. Spec. Pap. Geol. Soc. Am. 332, 365–384. https://doi.org/10.1130/0-8137-2332-9.365.
Schemmel, F., Niedermeyer, E.M., Schwab, V.F., Gleixner, G., Pross, J., Mulch, A., 2016. Plant wax δD values record changing Eastern Mediterranean atmospheric circulation patterns during the 8.2 kyr B.P. climatic event. Quat. Sci. Rev. 133, 96–107. https://doi.org/10.1016/j.quascirev.2015.12.019.
Scholz, C.A., Johnson, T.C., Cohen, A.S., King, J.W., Peck, J.A., Overpeck, J.T., Talbot, M.R., Brown, E.T., Kalindekafe, L., Amoako, P.Y.O., Lyons, R.P., Shanahan, T.M., Castañeda, I.S., Heil, C.W., Forman, S.L., McHargue, L.R., Beuning, K.R., Gomez, J., Pierson, J., 2007. East African megadroughts between 135 and 75 thousand years ago and bearing on early-modern human origins. Proc. Natl. Acad. Sci. Unit. States Am. 104, 16416–16421.
Shackleton, N.J., Opdyke, N.D., 1976. Oxygen-Isotope and Paleomagnetic Stratigraphy of Pacific Core V28-239 Late Pliocene to Latest Pleistocene. https://doi.org/10.1130/MEM145-p449.
Short, D.A., Mengel, J.G., Crowley, T.J., Hyde, W.T., North, G.R., 1991. Filtering of milankovitch cycles by earth's geography. Quat. Res. 35, 157–173. https://doi.org/10.1016/0033-5894(91)90064-C.
Stocker, T.F., Johnsen, S.J., 2003. A minimum thermodynamic model for the bipolar seesaw. Paleoceanography 18. https://doi.org/10.1029/2003PA000920.
Stockhecke, M., Kwiecien, O., Vigliotti, L., Anselmetti, F.S., Beer, J., Çağatay, M.N., Channell, J.E.T., Kipfer, R., Lachner, J., Litt, T., Pickarski, N., Sturm, M., 2014a. Chronostratigraphy of the 600,000 year old continental record of Lake Van (Turkey). Quat. Sci. Rev. 104, 8–17. https://doi.org/10.1016/j.quascirev.2014.04.008. Special Issue: Results from the PALEOVAN Drilling Project: a 600,000 year long continental archive in the Near East.
Stockhecke, M., Sturm, M., Brunner, I., Schmincke, H.-U., Sumita, M., Kipfer, R., Cukur, D., Kwiecien, O., Anselmetti, F.S., 2014b. Sedimentary evolution and environmental history of Lake Van (Turkey) over the past 600 000 years. Sedimentology 61, 1830–1861. https://doi.org/10.1111/sed.12118.
Sun, J., Huang, X., 2006. Half-precessional cycles recorded in Chinese loess: response to low-latitude insolation forcing during the Last Interglaciation. Quat. Sci. Rev. 25, 1065–1072. https://doi.org/10.1016/j.quascirev.2005.08.004.
Taner, M.T., 1992. Attributes revisited (Technical Report). Rock Solid Images, Inc.
Thomson, J., Nixon, S., Summerhayes, C.P., Schönfeld, J., Zahn, R., Grootes, P., 1999. Implications for sedimentation changes on the Iberian margin over the last two glacial/interglacial transitions from (230Thexcess)0 systematics. Earth Planet Sci. Lett. 165, 255–270. https://doi.org/10.1016/S0012-821X(98)00265-9.
Torrence, C., Compo, G.P., 1998. A practical guide to wavelet analysis. Bull. Am. Meteorol. Soc. 79, 61–78. https://doi.org/10.1175/1520-0477(1998)079<0061:APGTWA>2.0.CO;2.
Trauth, M.H., Deino, A.L., Bergner, A.G.N., Strecker, M.R., 2003. East African climate change and orbital forcing during the last 175 kyr BP. Earth Planet Sci. Lett. 206, 297–313. https://doi.org/10.1016/S0012-821X(02)01105-6.
Trauth, M.H., Larrasoaña, J.C., Mudelsee, M., 2009. Trends, rhythms and events in Plio-Pleistocene African climate. Quat. Sci. Rev. 28, 399–411. https://doi.org/10.1016/j.quascirev.2008.11.003.
Turney, C.S.M., Kershaw, A.P., Clemens, S.C., Branch, N., Moss, P.T., Keith Fifield, L., 2004. Millennial and orbital variations of El Niño/Southern Oscillation and high-latitude climate in the last glacial period. Nature 428, 306–310. https://doi.org/10.1038/nature02386.
Tzedakis, P.C., Hooghiemstra, H., Pälike, H., 2006. The last 1.35 million years at Tenaghi Philippon: revised chronostratigraphy and long-term vegetation trends. Quat. Sci. Rev., Critical Quaternary Stratigraphy 25, 3416–3430. https://doi.org/10.1016/j.quascirev.2006.09.002.
Ulfers, A., Zeeden, C., Wagner, B., Krastel, S., Buness, H., Wonik, T., 2022. Borehole logging and seismic data from Lake Ohrid (North Macedonia/Albania) as a basis for age-depth modelling over the last one million years. Quat. Sci. Rev. 276, 107295. https://doi.org/10.1016/j.quascirev.2021.107295.
Ünal-İmer, E., Shulmeister, J., Zhao, J.-X., Tonguç Uysal, I., Feng, Y.-X., Duc Nguyen, A., Yüce, G., 2015. An 80 kyr-long continuous speleothem record from Dim Cave, SW Turkey with paleoclimatic implications for the Eastern Mediterranean. Sci. Rep. 5, 13560. https://doi.org/10.1038/srep13560.
Verschuren, D., Sinninghe Damsté, J.S., Moernaut, J., Kristen, I., Blaauw, M., Fagot, M., Haug, G.H., 2009. Half-precessional dynamics of monsoon rainfall near the East African Equator. Nature 462, 637–641. https://doi.org/10.1038/nature08520.
Vogel, H., Wagner, B., Zanchetta, G., Sulpizio, R., Rosén, P., 2010. A paleoclimate record with tephrochronological age control for the last glacial-interglacial cycle from Lake Ohrid, Albania and Macedonia. J. Paleolimnol. 44, 295–310. https://doi.org/10.1007/s10933-009-9404-x.
Wagner, B., Vogel, H., Francke, A., Friedrich, T., Donders, T., Lacey, J.H., Leng, M.J., Regattieri, E., Sadori, L., Wilke, T., Zanchetta, G., Albrecht, C., Bertini, A., Combourieu-Nebout, N., Cvetkoska, A., Giaccio, B., Grazhdani, A., Hauffe, T., Holtvoeth, J., Joannin, S., Jovanovska, E., Just, J., Kouli, K., Kousis, I., Koutsodendris, A., Krastel, S., Lagos, M., Leicher, N., Levkov, Z., Lindhorst, K., Masi, A., Melles, M., Mercuri, A.M., Nomade, S., Nowaczyk, N., Panagiotopoulos, K., Peyron, O., Reed, J.M., Sagnotti, L., Sinopoli, G., Stelbrink, B., Sulpizio, R., Timmermann, A., Tofilovska, S., Torri, P., Wagner-Cremer, F., Wonik, T., Zhang, X., 2019. Mediterranean winter rainfall in phase with African monsoons during the past 1.36 million years. Nature 573, 256–260. https://doi.org/10.1038/s41586-019-1529-0.
Wagner, B., Vogel, H., Zanchetta, G., Sulpizio, R., 2010. Environmental change within the Balkan region during the past ca. 50 ka recorded in the sediments from lakes Prespa and Ohrid. Biogeosciences 7, 3187–3198. https://doi.org/10.5194/bg-7-3187-2010.
Wagner, B., Wilke, T., Krastel, S., Zanchetta, G., Sulpizio, R., Reicherter, K., Leng, M.J., Grazhdani, A., Trajanovski, S., Francke, A., Lindhorst, K., Levkov, Z., Cvetkoska, A., Reed, J.M., Zhang, X., Lacey, J.H., Wonik, T., Baumgarten, H., Vogel, H., 2014. The SCOPSCO drilling project recovers more than 1.2 million years of history from Lake Ohrid. Sci. Drill. 17, 19–29. https://doi.org/10.5194/sd-17-19-2014.
Wanner, H., Brönnimann, S., Casty, C., Gyalistras, D., Luterbacher, J., Schmutz, C., Stephenson, D.B., Xoplaki, E., 2001. North Atlantic oscillation – concepts and studies. Surv. Geophys. 22, 321–381. https://doi.org/10.1023/A:1014217317898.
Weedon, G.P., 2003. Time-Series Analysis and Cyclostratigraphy: Examining Stratigraphic Records of Environmental Cycles. Cambridge University Press.
Zeeden, C., Kaboth, S., Hilgen, F.J., Laskar, J., 2018. Taner filter settings and automatic correlation optimisation for cyclostratigraphic studies. Comput. Geosci. 119, 18–28. https://doi.org/10.1016/j.cageo.2018.06.005.